PHYSICAL REVIEW B VOLUME 27, NUMBER 5 1 MARCH 1983

Correlation theory for one dynamical variable: Application to EuO and EuS

Per-Anker Lindgård
Risø National Laboratory, DK-4000 Roskilde, Denmark*
and Oak Ridge National Laboratory, Oak Ridge, Tennessee 37830
(Received 27 August 1982)

A self-consistent correlation theory is developed which is a systematic generalization of the random-phase approximation and with an equally wide range of applicability. For simplicity the theory is here given in detail for one dynamical variable. For a test of the theory static and dynamic magnetic properties for EuO and EuS for $T \geq T_c$ are calculated. Quantitative agreement with the comprehensive and detailed experimental data is obtained for $T \geq 1.02T_c$ with no adjustable parameters. A dependence on the lattice and spin dimension as well as the value of the spin is obtained and is in agreement with high-temperature-expansion results.

I. INTRODUCTION

A theoretical framework in which one can calculate both static and dynamic properties accurately for a wide range of wave vectors q, frequencies ω, and temperatures T is useful in many areas of physics. The theory must be simple enough to make self-consistent calculations possible and also to make applications of realistic Hamiltonians possible. The only theory having these virtues is presumably the random-phase approximation (RPA),[1] in which the effect of many-body interactions is taken into account only as a static, wave-vector-dependent average field. It is valid when correlation effects are small; this condition can be evaluated by the RPA theory, yielding a kind of Ginzburg-Landau criterion for the range of applicability. When correlation effects are important, for example, near phase transitions T_c or in low dimensions, the accuracy of the RPA theory is not satisfactory either with respect to quantitative values of static properties or with respect to even qualitative features of dynamic properties, for example, when no damping of modes is obtained. It is the purpose of this paper to develop an interpolation theory which reduces to the correct limits at $T \to 0$ and $T \to \infty$ and also includes an essential part of the correlation effects, thereby being applicable at all temperatures and quite reliable near T_c. Of course if all correlations are not included one cannot expect to get exact results for T_c and the critical behavior. However, the dominant features can be obtained when including the correlations even in the lowest approximation and a Ginzburg-Landau criterion may be applied. The increase in the range of applicability relative to the RPA theory is considerable yielding damping and better temperature renormalization of modes, and for static properties a dependence of lattice dimensionality d, spin dimensionality n, and the length of the spin S, for magnetic Hamiltonians. The basic physical principle underlying this correlation theory (CT) is to calculate static properties using exact relations in terms of approximate, but realistic dynamic properties, i.e., including damping and renormalization; the whole calculation is made self-consistent by making use of the mode-mode coupling approximation for the damping parameters. Mori and Kawasaki[2] have developed formal generalizations of the RPA theory in terms of slowly varying thermodynamic variables and relaxation functions. However, in their approach the static properties are not calculated but assumed to be known *ab initio*. Furthermore, no prescription is given on how to define the proper thermodynamic variables. The whole physical content of these exact theories is in fact hidden in the choice of these variables. In this paper we use a Green's-function approach which yields the static susceptibility and also specifies the dynamical variables.

Another purpose of the present paper is to formulate a theoretical framework which can be straightforwardly generalized to complicated many-body problems which have traditionally only been tractable by the RPA theory. A proximate problem is, for example, that of the general anisotropic magnetic system of spins interacting with anisotropic forces and subject to anisotropic crystal fields.[3] The crystal-field problem is an example of the more general class of problems of interacting objects with internal degrees of freedom.

However, it is important first to test the range of applicability of the correlation theory on the well-

studied Heisenberg-model system, which in the paramagnetic phase only has one dynamical variable $A_q = S_q^z$. Several particular theories have been developed for this case: de Gennes,[3] Resibois and de Leener,[4] Mori and Kawasaki,[2] Tomita and Mashiyama,[5] Blume and Hubbard,[6] Lovesey and Meserve,[7] etc. It is not our intent to go beyond these theories in accuracy, but to formulate theory which can be more easily generalized and applied to more complicated cases.

Experimentally EuO and EuS represent the best-known examples of the Heisenberg system, the relatively weak dipolar interaction can be neglected in the paramagnetic phase. The lattice structure is fcc and there are essentially only nearest- and next-nearest-neighbor exchange interactions. For EuO (Ref. 8) they are both ferromagnetic $J_1 = 0.625$ K and $J_2 = 0.125$ K, but for EuS (Ref. 9) there are competing interactions $J_1 = 0.253$ K and $J_2 = -0.096$ K. This gives rise to interesting differences in the paramagnetic phase. For the other chalcogenides the competing feature is predominant[10]: for EuSe, $J_2/J_1 \sim -1$ and for EuTe, $J_2/J_1 \sim -2$. In these systems the dipolar interactions play a more important role; they will be discussed elsewhere. A brief account of the results of the CT applied to EuO and EuS was given previously.[11] Subsequently Young and Shastry[12] made a similar analysis using the spherical model for the static properties and the Lovesey-Meserve theory for the dynamic properties.

The organization of the paper is as follows. In Sec. II the theoretical scheme for one dynamical variable is presented. In Secs. III and IV a detailed comparison between the existing extensive theoretical and experimental material and the present theory is made. The last section discusses the results, and some technical details are provided in the appendixes.

II. CORRELATION THEORY FOR ONE DYNAMICAL VARIABLE: HEISENBERG SYSTEM FOR $T > T_c$

The CT for one dynamical variable A_q is particularly simple. The Heisenberg system in the paramagnetic phase is an example of this case which we will discuss in order to be explicit. Since there is full symmetry between S^x, S^y, and S^z we may choose $A_q = S_q^z$ as the dynamical variable. Let us consider the Heisenberg Hamiltonian,

$$H = -\sum_{ij} J_{ij} \vec{S}_i \cdot \vec{S}_j = -\frac{1}{N} \sum_q J_q \vec{S}_q \cdot \vec{S}_q \ . \tag{1}$$

We wish to derive $\chi_q(\omega)$, the dynamical susceptibility using the Green's-function formalism. In order to proceed beyond the RPA decoupling we use an exact decoupling approach closely related to the projection-operator formalism developed by Mori[2] and express the equations of motions in terms of the exact frequency moments involving $\langle S_q^z \rangle, \langle S_q^\alpha S_q^\alpha \rangle$ where $\alpha = x,y,z$, and the remainder, which is expressed as a memory function. The memory function is formulated as a relaxation function, which may be decoupled in the mode-mode coupling approximation. This method has been intensively used in the theory of dynamic critical phenomena, in particular by Kawasaki.[2] The advantage of using the Green's-function formalism combined with the decoupling approach is that then one directly obtains results for both the dynamic and the static susceptibilities. In theories using the normalized relaxation functions and the Mori projection operators, the static quantities are supposed to be known *ab initio* and only the dynamics can be derived.

Let us consider the equation of motions to second order for the Zubarev[1] Green's functions,

$$G_0(t) = \langle\langle A(t); A^\dagger(0) \rangle\rangle = -i\theta(t) \langle [A(t), A^\dagger] \rangle \ ,$$

where A and $A^\dagger$ represent the spin operators S_q^+, S_q^-, or S_q^z. The corresponding relaxation function is defined as

$$(A(t) A^\dagger) = \int_0^\infty d\lambda \langle e^{\lambda H} A(t) e^{-\lambda H} A^\dagger \rangle - \langle A \rangle \langle A^\dagger \rangle \ .$$

The Fourier-transformed exact equations of motion can be written as follows:

$$\begin{aligned} &(\omega + a_{10}) G_0(\omega) + G_1(\omega) = b_{10} \ , \\ &(a_{10}\omega + a_{20}) G_0(\omega) + (\omega + a_{21}) G_1(\omega) \\ &\qquad + G_2(\omega) = b_{20} \ , \end{aligned} \tag{2}$$

or by eliminating $G_1(\omega)$,

$$\begin{aligned} &(\omega^2 + \omega a_{21} + a_{21} a_{10} - a_{20}) G_0(\omega) - G_2(\omega) \\ &\qquad = b_{10}(\omega + a_{21}) - b_{20} \ , \end{aligned} \tag{3}$$

where a_{lm} and b_{l0} are frequency-independent constants and the higher-order Green's functions are defined as

$$G_n(\omega) = \frac{1}{2\pi} \int_{-\infty}^{\infty} \langle\langle X_n(t); A^\dagger \rangle\rangle e^{i\omega t} dt \ , \tag{4}$$

where the random-force operator $X_n(t)$ is the remainder of the nth time derivative of $A(t)$ after the regular precession is projected out. Using the Liouville operator L to represent the time derivative

$$LA(t) = [H, A(t)] = -i dA(t)/dt$$

one writes

$$LA(t)=a_{10}A(t)+X_1(t)\ ,$$
$$L^2A(t)=a_{20}A(t)+a_{21}X_1(t)+X_2(t)\ . \tag{5}$$

In order to make (5) true for all t we must consider the time dependence of $X_1(t)$ in a moving frame corresponding to the regular precession. The decoupling (5) is exact and the coefficients a_{lm} are related to the exact frequency moments of the relaxation function. Using the Mori projection operator one has

$$a_{10}=(LAA^\dagger)/(AA^\dagger)_{t=0}=-\langle\omega_q\rangle\ ,$$
$$a_{20}=(L^2AA^\dagger)/(AA^\dagger)_{t=0}=\langle\omega_q^2\rangle\ , \tag{6}$$
$$a_{21}=(L^2AX_1^\dagger)/(XX_1^\dagger)_{t=0}$$
$$=(\langle\omega_q^3\rangle-\langle\omega_q^2\rangle\langle\omega_q\rangle)/(\langle\omega_q^2\rangle-\langle\omega_q\rangle^2)\ .$$

The constants

$$b_{10}=-\frac{1}{2\pi}\langle[L^{l-1}A,B]\rangle$$

are the thermal averages

$$b_{10}=-\frac{1}{2\pi}\langle S^z\rangle\ ,$$
$$b_{20}=-\frac{1}{2\pi}\sum_k 4(J_k-J_{k-q})\langle S_k^zS_{-k}^z\rangle\ . \tag{7}$$

In the paramagnetic case $a_{10}=a_{21}=b_{10}=0$, this shows the necessity of going to second order in the equations of motion. We notice that in the RPA theory only the equation of motion (5) to first order is used, $G_1(\omega)$ is neglected in Eq. (2), and a decoupling approximation is introduced for the first moment a_{10} giving

$$\langle\omega_q\rangle=2\langle S^z\rangle(J_0-J_q)\ .$$

The RPA theory is therefore not applicable in the disordered phase. Using the exact relation

$$\langle\langle X_2;A^\dagger\rangle\rangle_{\omega=0}=-2\pi(X_2A^\dagger)_{t=0}\ ,$$

and the fact that by definition the projection of X_2 on $A^\dagger$ is zero, it follows that $G_2(\omega=0)\equiv 0$. At $\omega=0$ it is therefore exact to neglect $G_2(\omega)$ from the equation of motions (3). This can be utilized to find solutions valid for small frequencies (see Appendix A). To lowest order one obtains a two-pole solution for $G_0(\omega)$ of the form

$$G_0(\omega)=\chi_q\langle\omega_q^2\rangle \times\frac{1}{2\pi}\frac{1}{(\omega-\alpha_q-i\beta_q)(\omega+\alpha_q-i\beta_q)}\ , \tag{8}$$

where $\alpha_q^2+\beta_q^2=\langle\omega_q^2\rangle$. This solution yields the exact zeroth and second moments self-consistently, i.e., χ_q and $\langle\omega_q^2\rangle$; the damping parameter β_q is related to the random force relaxation function $(X_1X_1^\dagger)$, to be discussed below. The two-pole solution has, in fact, a simple physical interpretation. If we consider the Green's function $\langle\langle S_q^+;S_{-q}^-\rangle\rangle$, it has at $T=0$ only a pole at the spin-wave frequency $\omega=\omega_{SW}$. A spin flip, therefore, corresponds to the creation of a spin wave in a fully ordered state with spin up, say. In the disordered phase the fluctuations yield equally many small correlated regions with spin up and spin down, and a spin flip then corresponds to either creation or destruction of short-lived spin waves, i.e., resonances at both $\omega=\alpha+i\beta$ and at $\omega=-\alpha+i\beta$.

We can now discuss the determination of static properties. Since by definition $-2\pi G_0(\omega=0)$ is equal to the static susceptibility, we have exactly from (3) and (7),

$$\chi_a=-2\pi b_{20}/a_{20}$$
$$=\frac{4}{\langle\omega_q^2\rangle}\sum_k(J_k-J_{k-q})\langle S_k^zS_{-k}^z\rangle\ . \tag{9}$$

For small q one may expand in q and write

$$\chi_q\sim 1/(\kappa_1^2+q^2)\ .$$

This defines the correlation length $\xi=\kappa_1^{-1}$. The static correlation function is obtained from the exact relation

$$\langle S_q^zS_{-q}^z\rangle=\int_{-\infty}^{\infty}\frac{\mathrm{Im}G_0(\omega)}{1-e^{-\omega/kT}}d\omega\ . \tag{10}$$

It is insensitive to details in the line shape and is exact in the high-temperature-expansion sense when the first several moments are exact. Because

$$\langle S_x^2+S_y^2+S_z^2\rangle=S(S+1)\ ,$$

the following normalizing condition must be fulfilled:

$$S(S+1)/3=\frac{1}{N}\sum_k\langle S_k^zS_{-k}^z\rangle\ . \tag{11}$$

The real-space correlation functions are, by definition,

$$\langle S_0S_{R_n}\rangle=\frac{1}{N}\sum_k\gamma_k^{(n)}\langle S_k^zS_{-k}^z\rangle\ , \tag{12}$$

where

$$\gamma_k^{(n)}=\sum_{R_n}\exp(ikR_n)/z_n$$

is the sum over the nth group of neighbors with z_n members. It is clear from (9) that $\chi_q\langle\omega_q^2\rangle$ is proportional to $\langle S_0S_R\rangle$ for a particular wave vector q. This relation is simpler to use than (12) directly.

The determination of the dynamical properties proceeds as follows. For finite frequencies $G_2(\omega)$ cannot be neglected and it is advantageous to express $G_2(\omega)$ as a memory function times $G_0(\omega)$ before approximations are introduced. This is discussed in Appendix A. The exact formal solution by Mori for the Laplace-transformed relaxation function is a convenient starting point for approximations,

$$(S_q^z \mid S_{-q}^z)_z = \int_0^\infty (A(t) \mid A^\dagger) e^{-zt} dt = \frac{\chi_q}{z + (X_1 X_1^\dagger)_z}, \quad z = i\omega \ . \tag{13}$$

However, two problems must be solved before (13) can be considered useful. In the following approximation scheme, which we shall refer to as CT, a systematic and general method to self-consistently include pair-correlation effects is presented.

The first problem is finding a realistic frequency dependence for $(S_q^z S_{-q}^z)_z$. Guided by solution (8) for the Green's function near $\omega = 0$ and the physical interpretation that the two poles correspond to damped spin-wave excitations, we expect that the two-pole approximation for (13) yields a realistic parametrization of the frequency dependence for frequencies on the scale of the spin-wave frequency. The two-pole solution corresponds to assuming a single relaxation time $(2\beta)^{-1}$ for $(X_1 X_1^\dagger)_t$ and writing

$$(X_1 X_1^\dagger)_z = \chi_q \langle \omega_q^2 \rangle \frac{1}{z + 2\beta_q} \ . \tag{14}$$

The corresponding line-shape function is $S(q,\omega) = \mathrm{Im} G_0(\omega)/\omega$,

$$S(q,\omega) = \frac{1}{\pi} \chi_q \langle \omega_q^2 \rangle \frac{\beta_q}{(\omega^2 - \langle \omega_q^2 \rangle)^2 + 4\beta_q^2 \omega^2} \quad \text{for } \omega \lesssim \omega_c \ . \tag{15}$$

For large ω the damped harmonic oscillator form (15) has wings that are clearly too large. The simplest remedy is to introduce a cutoff at large frequencies $\omega = \omega_c$, determined such that $\langle \omega_q^4 \rangle$ is correct. This ensures that all higher moments are also finite. This is a generalization of the approach by de Gennes,[3] who assumed a cutoff Lorentzian line shape for (15). The effects of introducing the cutoff are described in Appendix B. The next problem is to express $(X_1 X_1^\dagger)_z$ in known quantities. Since a_{10} is zero for $T > T_c$, $X_1(t) = LA(t)$, and

$$(X_1(t) \mid X_1^\dagger) = (\dot{S}_q^z(t) \mid \dot{S}_{-q}^z) = 4 \sum_{kk'} (J_k - J_{k-q})(J_{k'} - J_{k'-q}) (S_k^x(t) S_{q-k}^y(t) \mid S_{-k'k'-q}^{x\,y}) \ . \tag{16}$$

Using an approximate decoupling of the x and y modes and the full symmetry between x, y, and z we then have

$$(X_1 \mid X_1^\dagger)_z = 4kT \sum_k (J_k - J_{k-q})^2 \int (S_k^z S_{-k}^z)_{z'} (S_{q-k}^z S_{k-q}^z)_{z-z'} \frac{dz'}{2\pi i} \ . \tag{17}$$

Under the sum over k and the integral over z' the precise frequency dependence of $(S_k^z S_{-k}^z)_z$ is not important. It is therefore justified to approximate (17) further by simply using a Lorentzian line shape for

$$(S_k^z S_{-k}^z)_z \sim \chi_k / (z + \Gamma_k)$$

with the same area and halfwidth as the cutoff two-pole line shape. The halfwidth frequency is given by

$$\Gamma_k^2 = \alpha_k^2 - \beta_k^2 + [2(\alpha_k^4 + \beta_k^4)]^{1/2}, \quad \alpha_k^2 = \langle \omega_k^2 \rangle - \beta_k^2 \ . \tag{18}$$

Using (14) and (17) one then has the following equation for the self-consistent determination of β_q and thereby of $(X_1 X_1^\dagger)_z$. We write

$$\frac{\chi_q \langle \omega_q^2 \rangle}{z + 2\beta_q} = 4kT \sum_k (J_k - J_{k-q})^2 \chi_k \chi_{k-q} \frac{1}{z + \Gamma_k + \Gamma_{q-k}} \Bigg|_{z=\Gamma_q} \ . \tag{19}$$

It is clear from (14) and (15) that when the characteristic frequency Γ_q is much smaller than $2\beta_q$, $(X_1 X_1^\dagger)_z$ is nearly constant in the frequency range of interest for $(S_q^z S_{-q}^z)_z$. We therefore shall require that (17) or (19) is fulfilled for $z = \Gamma_q$. The above procedure breaks down if β_q becomes too small; this can be tested *a posteriori*. Equation (17) or (19) gives, by integration over the frequency,

$$\langle \omega_q^2 \rangle = \frac{4kT}{\chi_q} \sum_k (J_k - J_{k-q})^2 \chi_k \chi_{k-q} \ , \tag{20}$$

which in combination with the exact relation (9), allows a determination of the susceptibility χ_q by the same decoupling as used for the dynamical properties. Finally we need to calculate $\langle \omega_q^4 \rangle$. For short-range exchange interactions it is advantageous to

calculate $\langle\omega_q^4\rangle$ approximately using a decoupling of four spin-correlation functions[13] in real space and calculate the resulting pair-correlation functions by means of (12). More details are given in Appendix B.

The exchange interaction may be written

$$J_q \equiv J_0 \sum_n r_n \gamma_q^{(n)} , \tag{21}$$

where $J_0 = \sum_n z_n J_n$ is the sum over all interactions and $r_n = J_n/J_0$ is the relative contribution of the interaction with the neighbor group with z_n spins. For cubic, hexagonal, and several other lattices the following important relation is true for an arbitrary function F_k of k:

$$\sum_k (J_k - J_{k-q}) F_k = J_0 \sum_{k,n} (1-\gamma_q^{(n)}) r_n \gamma_k^{(n)} F_k . \tag{22}$$

Finally, for the self-consistent solutions of (19) and (20) it is convenient to use a functional form for the wave-vector dependence of χ_q and β_q. Analysis of (20) shows that we obtain the exact wave-vector dependence given by (9) for $\chi_q\langle\omega_q^2\rangle$, when χ_q has the RPA functional form

$$\chi_q = \frac{A}{B - J_q} , \tag{23}$$

where A and B are to be determined by self-consistent solutions of Eqs. (9)–(11), (19), and (20). Since the detailed dynamics, i.e., the value of β_q, plays a subordinate role for the static properties, the dynamic corrections entering in Eq. (10) can be introduced by an iteration procedure. The first iteration corresponds to the spherical approximation, i.e., replacing (10) by $\langle S_q^z S_{-q}^z\rangle \approx kT\chi_q$. It is, however, important to include the dynamic corrections to obtain accurate values for A and B particularly near T_c. All static properties and the moments can now be calculated for a given β_q.

The wave-vector dependence for the damping parameter β_q was for the fcc lattice found to be well represented by a Fourier expansion

$$\beta_q^2 = \sum_{n=0}^{3} b_n (1-\gamma_q^{(1)})^n , \tag{24}$$

where b_n are temperature-dependent constants which can be solved in terms of the static properties by considering four different wave vectors of Eq. (19). Expansion (24) is general, but other forms may be more rapidly converging. Near T_c it may be better to expand β_q^{-2} as (24). Such an expansion is similar to (23) for χ_q. However, with the use of (24) only a few iterations are required for obtaining the self-consistent static and dynamic properties in particular for temperatures not too close to T_c.

This completes the description of the scheme of approximations. It is, without loss of accuracy, simpler than previous schemes mainly because of the use of the two-pole approximation (8) and the parametrization (24) which makes the simultaneous self-consistency calculation of static and dynamic properties possible. It is also simple to generalize to systems with more than one dynamical variable. The singlet-doublet problem for $S=1$ has nine dynamical variables; this problem will be discussed in a separate paper.[14]

In recent years it has been very popular to discuss dynamic properties using the Ginzburg-Landau theory.[15] This amounts to solving the generalized Langevin equation for a thermodynamic variable A,

$$m\ddot{A} + \gamma\dot{A} = f(t) - \frac{\partial F}{\partial A} , \tag{25}$$

where $f(t)$ is a random force, the last term is a thermodynamic force, and m and γ are phenomenological constants assumed to be slowly varying with temperature. The problem focused on in the Ginzburg-Landau theory is the influence of the static properties on the dynamic properties. The static properties represented by the free energy F are supposed to be known *ab initio*. For small A one may write

$$\frac{\partial F}{\partial A} = \frac{A\partial^2 F}{\partial A^2} = \chi A .$$

Equation (25) is, in fact, exactly equivalent to the Mori continued fraction to second order, i.e., the two-pole approximation. In this light the CT is a bridge between the Ginzburg-Landau and the Mori theory, providing additionally a simple scheme for calculating the static properties F and the dynamical properties m and γ self-consistently. The methods developed for discussing the Ginzburg-Landau theory are, of course, useful for getting a good starting point for the iterative solutions searched for in the CT. In the following sections the accuracy of the CT is tested.

III. HEISENBERG MODEL IN DIFFERENT LATTICE DIMENSIONS d

For nearest-neighbor interaction J, the Heisenberg model has been studied intensively theoretically by many methods. There are no experimental realizations of this case. In Fig. 1 we show the uniform static susceptibility calculated by the CT for $S=1$. The transition temperature T_c is for the three-dimensional (3D) fcc lattice found to be 2% lower than that obtained by the high-temperature expansion (16) for $S=1$ which probably is within the ac-

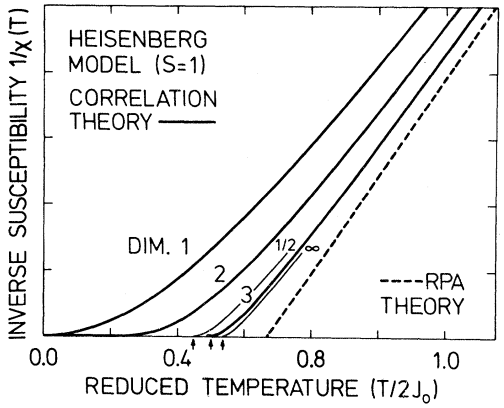

FIG. 1. Calculated inverse static susceptibility at $q=0$ for lattice dimension $d=1$, 2, and 3. Full lines are for $S=1$. Thin lines are for $S=\frac{1}{2}$ and $S=\infty$ for $d=3$. Arrows indicate the results of high-temperature expansions (Ref. 16).

curacy of the latter. By thin lines we also indicate $1/\chi_0$ for $S=1/2$ and $300-\infty$. The scale is such that they are identical at $T=\infty$. The agreement is excellent with the high-temperature-expansion results for T_c indicated by arrows. We also notice that although the asymptotic value of $1/\chi_0$ is identical to the RPA value for $T=\infty$ there is a substantial difference at temperatures much larger than T_c. This is again in agreement with the results found by the high-temperature expansions.

IV. HEISENBERG MAGNETS EuO AND EuS

The best experimental realizations of the Heisenberg model are EuO (Ref. 8) and EuS (Ref. 9) in which there are both nearest-neighbor (NN) and also significant next-nearest-neighbor (NNN) interactions. We include the isotropic part of the dipolar interactions. Interactions to more distant neighbors are small and of the order of the dipolar interaction; these interactions are neglected in the following.

A. Self-consistent calculation of static properties

Using the exchange parameters J_1 and J_2 the calculated transition temperatures are shown in Table

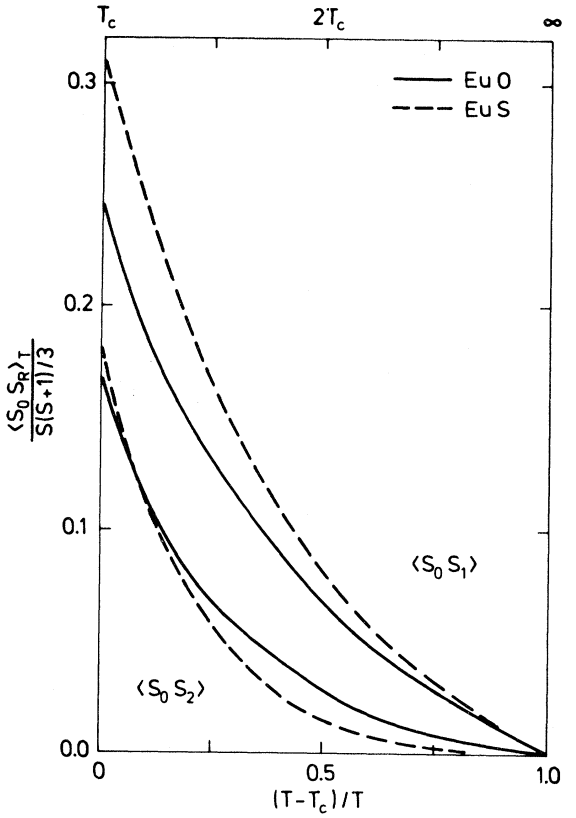

FIG. 2. Calculated normalized nearest neighbor and next-nearest neighbor correlations as a function of temperature.

I. We obtain agreement with the observed T_c within a few K. The deviation is of the magnitude expected from the dipolar interactions. The contribution to T_c estimated from the NN and NNN isotropic part is 3 and 2 K for EuO and EuS, respectively. We notice that the CT gives a substantial reduction of T_c relative to the mean field T_c^{MF}. The reduction is larger for EuS because of the competing interactions $J_1>0>J_2$. A consequence of this shows up in the short-range correlation functions shown in Fig. 2. The NN correlation $\langle S_0S_1\rangle$ is larger for EuS than for EuO at T_c, because T_c is relatively lower. The NNN correlation $\langle S_0S_2\rangle$ is smaller because of the negative sign of J_2. However, J_2 is not large enough to make $\langle S_0S_2\rangle$ change sign as a function of temperature at a so-called disorder point.[16] EuSe

TABLE I. Calculated and measured transition temperatures.

	T_c (mean field) (K)	T_c (CT) (K)	T_c (expt)[a] (K)	T_c (CT)/T_c (mean field)
EuO	86.6	66.6	69.1	0.768
EuS	25.8	17.1	16.6	0.662

[a]Reference 8.

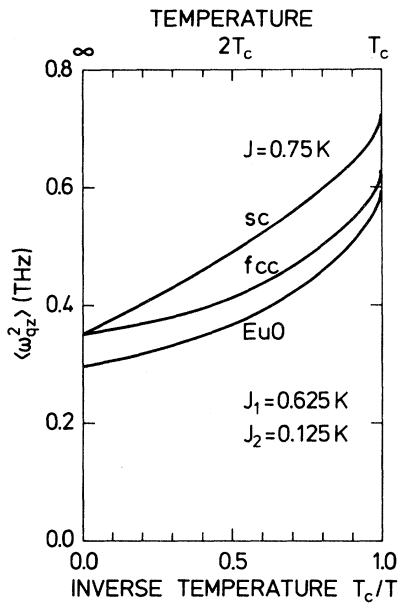

FIG. 3. Calculated second moment as a function of temperature for EuO and for nearest-neighbor sc and fcc lattices. Choosing $J=J_1+J_2=0.75$ K equalizes the (111) zone-boundary spin-wave energies at $T=0$.

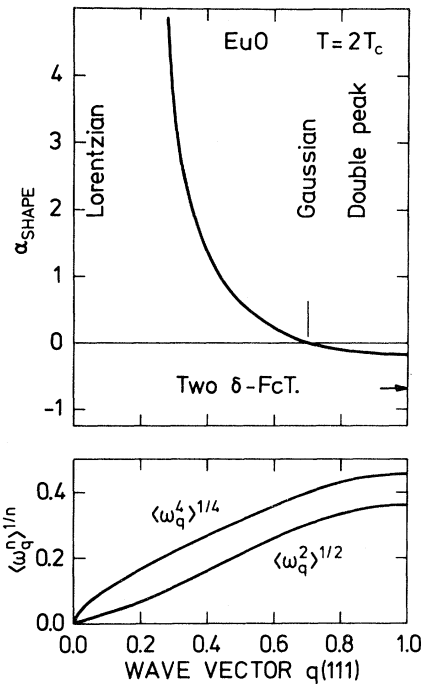

FIG. 4. Line-shape parameter $\alpha=\langle\omega_q^4\rangle/3\langle\omega_q^2\rangle^2-1$ and comparison between the calculated moments $\langle\omega_q^4\rangle^{1/4}$ and $\langle\omega_q^2\rangle^{1/2}$ for q along (111).

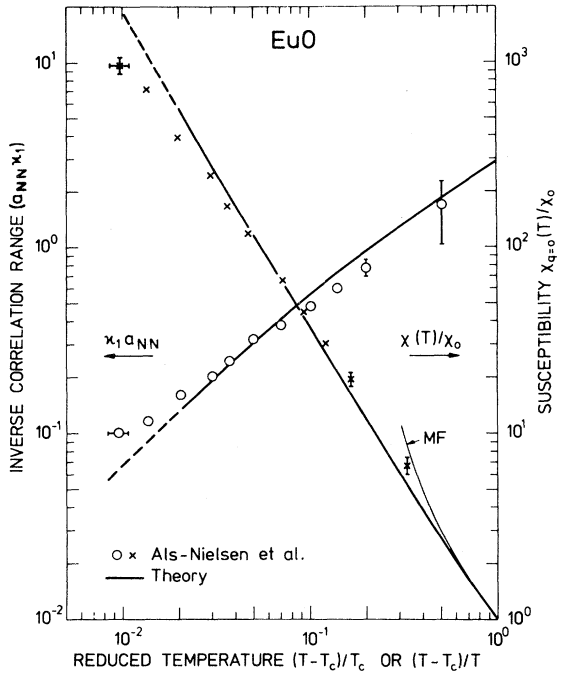

FIG. 5. Calculated reduced susceptibility $\chi_{q=0}(T)/\chi_0$ for EuO as a function of $(T-T_c)/T$ compared with scaled experimental data (Ref. 8). Mean-field susceptibility (MF) is also indicated. Calculated inverse correlation range κ_1 multiplied by the nearest-neighbor distance a_{NN} agrees with no adjustable parameters with the measured points (Ref. 8) down to $(T-T_c)/T_c=0.02$.

and EuTe are better candidates for this effect. The calculated temperature dependence of the second moment $\langle\omega_q^2\rangle$ for q at the (111) zone boundary is shown in Fig. 3 for EuO and for NN-model sc and fcc lattices with $J=0.75$ K, which gives the same (111) zone-boundary spin wave at $T=0$. The second moment depends on J_1^2 and J_2^2, and therefore $\langle\omega_q^2\rangle$ is much smaller for real EuO than for a NN model with $J=J_1+J_2$. This is the main reason for the discrepancy between the dynamic calculations for the sc lattice by Hubbard[6] and EuO. In Fig. 4 the magnitudes of $\langle\omega_q^4\rangle^{1/4}$ and $\langle\omega_q^2\rangle^{1/2}$ are shown for EuO at $T=2T_c$ for q along the (111) direction. Although the difference does not appear to be large, the line-shape parameter[13]

$$\alpha=\langle\omega_q^4\rangle/3\langle\omega_q^2\rangle^2-1$$

varies dramatically from ($\alpha=\infty$) given a Lorenztian line shape for small q to ($\alpha<0$) giving a double-peak line shape at large q. We notice by comparing Figs. 2 and 4 that the double peak appears despite the fact that short-range correlations are quite small, i.e., less than 10% of the maximum value $S(S+1)/3$. The correlated regions are far from well

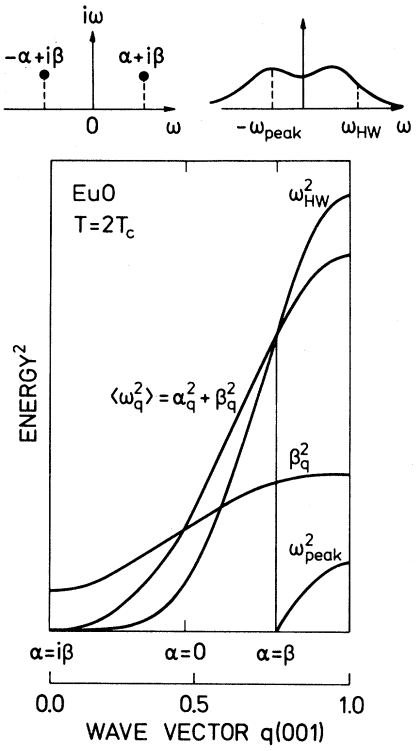

FIG. 6. Two-pole line shape and parameters $\pm\alpha+i\beta$. Calculated $\langle\omega_q^2\rangle$, β_q^2, ω_{HW}^2, and ω_{peak}^2, where ω_{HW} is the halfwidth at full maximum frequency and ω_{peak} is the peak-value frequency. For $T>T_c$, $\omega_{\mathrm{HW}}^2\sim q^4$, whereas $\langle\omega_q^2\rangle\sim q^2$. At T_c, $\omega_{\mathrm{HW}}^2\sim q^5$, in agreement with dynamical scaling.

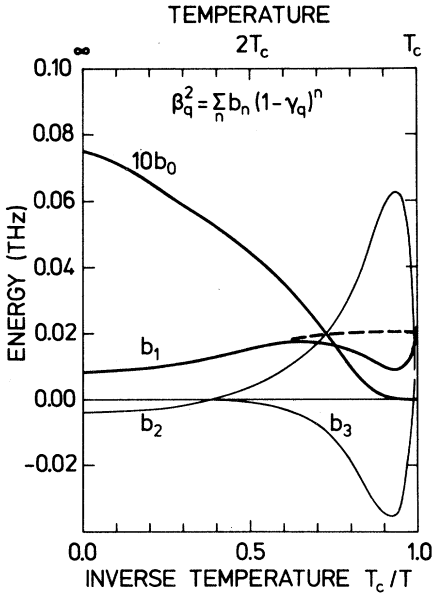

FIG. 7. Calculated temperature dependence of the parameters determining the damping parameters β_q in Eq. (24).

defined. Figure 5 shows the calculated reduced susceptibility $\chi_{q=0}(T)/\chi_0$ where

$$\chi_0=S(S+1)/3kT\ .$$

The agreement with the experimental points (scaled) is satisfactory for $(T-T_c)/T$ larger than 2%. The comparison between the calculated and measured correlation length κ_1 involves no adjustable parameters. Again the agreement is satisfactory for $(T-T_c)/T_c$ larger than 2%. The difference between EuO and EuS is small for these quantities. It is possible that dipolar effects become important for temperatures within 2% of T_c.[17]

B. Self-consistent calculation of dynamic properties

Given the calculated $\langle\omega_q^2\rangle$ and $\langle\omega_q^4\rangle$ as a function of temperature it now remains to calculate the line shape in more detail than given by the qualitative arguments shown in Fig. 4. For this purpose we use the cutoff two-pole approximations. The only parameter to calculate is then the inverse relaxation time for the random forces $2\beta_q$. This is found using representation (24) and solving (19). Figure 6 shows the wave-vector dependence along the (001) direction of $\langle\omega_q^2\rangle$,β_q^2, and the frequency at half maximum ω_{HW}^2 for $T=2T_c$ in EuO when we neglect the cutoff correction. There are poles at $\pm\alpha+i\beta$. When $q\to 0$ we find that because $\alpha\to i\beta$ the halfwidth frequency decreases more rapidly than the second moment such that $\omega_{\mathrm{HW}}=Dq^2$. Since the line shape then is nearly Lorentzian this means a diffusional behavior at small q for $T>T_c$. However, near T_c, $\beta_{q=0}\to 0$, so both poles go to zero and one finds dynamical scaling $\omega_{\mathrm{HW}}\sim q^{5/2}$; this is; of course, well known in the mode-mode coupling approximation.[2] The temperature dependence of the parameters b_n is shown on Fig. 7. The constant b_0 is well determined for different temperatures. Near T_c the wave-vector dependence of β_q varies strongly with temperature. With expansion (24) there is a substantial correlation between the parameters in particular between b_2 and b_3. Near T_c it may be better to Fourier expand β_q^{-2}. The qualitative features obtained with the simple two-pole approximation are correct without calculating $\langle\omega_q^4\rangle$. At large q a peak appears at $\omega=\omega_{\mathrm{peak}}$ when $\alpha_q>\beta_q$. In this region $\langle\omega_q^2\rangle$ is a good measure for the halfwidth. On an absolute scale the linewidth calculated by the pure two-pole approximation is too narrow by about 40%. The reason is that the wings contribute too much to the second moment. By introducing a cutoff of the wings so that also $\langle\omega_q^4\rangle$ is obtained correctly (see Appendix B) the halfwidth ω_{HW} increases by 40%. A comparison in Fig. 8 between the calculated and measured

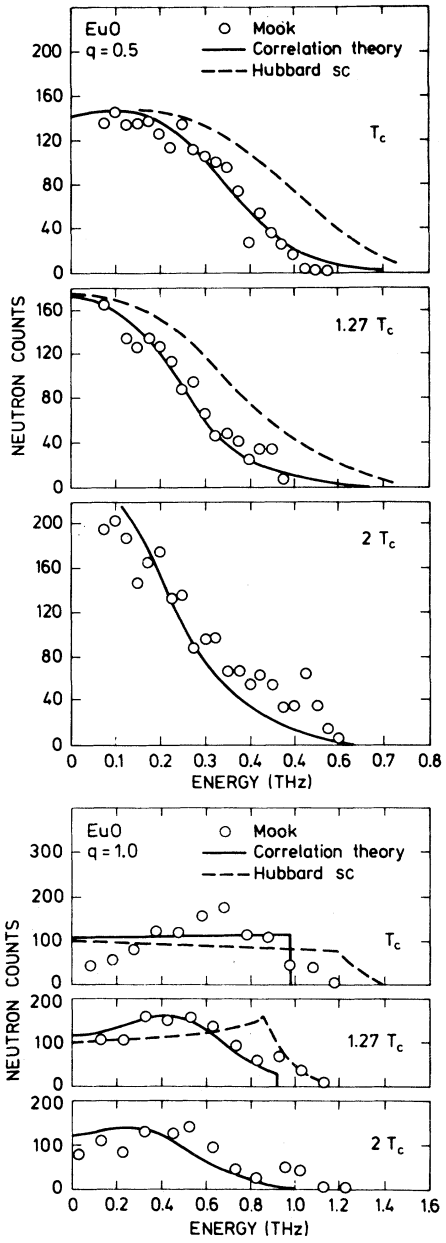

FIG. 8. Calculated and measured (Ref. 18) line shapes for EuO at $T=1$, 1.27, and $2T_c$. Dashed line indicates the effective nearest-neighbor model calculated by Hubbard (Ref. 6).

line shape for EuO (Ref. 18) shows excellent agreement for $q=0.5q_{\text{zone}}$ (111) for $T=T_c$, $1.3T_c$, and $2T_c$. At the zone boundary the cutoff becomes important near T_c, but the agreement is again good for $T=1.3T_c$ and $2T_c$. Figure 9 shows a comparison between the calculated halfwidth ω_{HW} and peak position for EuO and EuS. The influence of the change of sign of J_2 is evident. For EuS the peak in the (111) direction only appears close to T_c and in

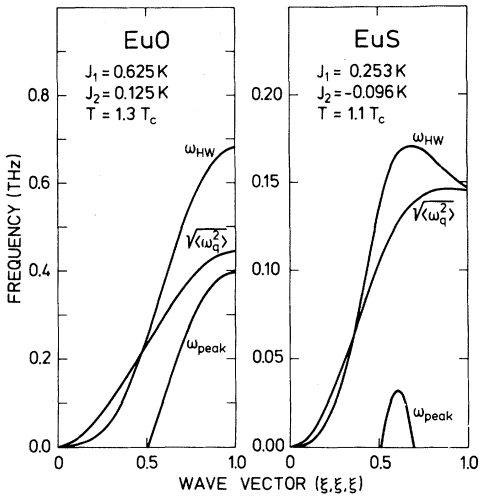

FIG. 9. Influence of J_2 is evident when comparing the calculated ω_{HW}, $\langle\omega_q^2\rangle^{1/2}$, and ω_{peak} for EuO and EuS as a function of $q(111)$.

the middle of the zone. In fact the dispersion curve resembles that for an antiferromagnet compared with the ferromagneticlike one for EuO. In the (001) direction the behavior of EuS is similar to that for EuO because the spin waves are higher in energy in this direction. This is in agreement with experiments.[9] For small q the line shape is Lorentzian and the calculated and experimental diffusion constant Λ_T are compared as a function of temperature on Fig. 10. For $T=T_c$ and small q a calculation of ω_{HW} gives dynamical scaling behavior for $q<0.1q_{\text{zone}}$ shown on Fig. 11. The calculated and experimental points are in reasonable agreement up to $0.2q_{\text{zone}}$, where the theory curves away and agrees with the halfwidth measured at $q=0.5q_{\text{zone}}$. The discrepancy between theory and experiment may be due to the fact that in the quite involved unfolding of the experimental results from resolution effects a Lorentzian line shape was assumed[8]. It has been shown here that significant deviations from this occurs for finite wave vectors.

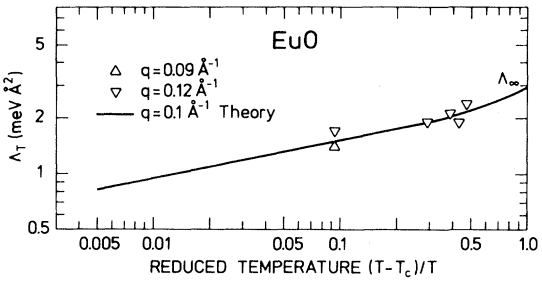

FIG. 10. Spin-diffusion constant Λ_T calculated at $q=0.1$ Å^{-1} compared with the measured (Ref. 8) Λ_T as a function of temperature.

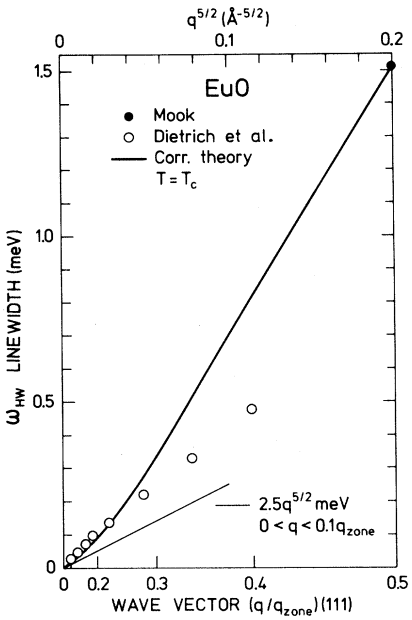

FIG. 11. Linewidth at $T=T_c$. Dynamical scaling, $\omega_{HW}\sim q^{5/2}$, is found for $q<0.1q_{zone}$. Experimental data (○) by Dietrich *et al.* (Ref. 8) appears to fulfill dynamical scaling to $0.4q_{zone}$, but seems not to agree with the data by Mook (Ref. 18) at $q=0.5q_{zone}$.

V. DISCUSSION

The CT includes, beyond the average effect considered by the RPA theory, the effects of pair correlations, which are introduced in a systematic way. In the theory, sum rules and a number of frequency moments $\langle\omega_q^n\rangle$ for $n<6$ are fulfilled exactly (self-consistently), and all higher moments ($n>6$) are finite and approximately correct. The moments basically contain information on high-frequency properties. In addition exact information about small-frequency properties are also fulfilled in the theory. The theory describes the lattice- and spin-dimensionality dependence and spin dependence of the NN Heisenberg model in good agreement with the best available alternative theories.[3–7] For the NNN Heisenberg model the theory is in agreement with a large amount of detailed experimental results for EuO and EuS with no adjustable parameters both for static and dynamic properties for all q, ω, and T. The limit for the global applicability of the correlation theory based on this comparison is $T\geq 1.02T_c$, or until the correlation length is about ten lattice spacings. For small q the dynamic properties are correctly described even at T_c. EuO and EuS have recently also been analyzed[12] in terms of the continued-fraction theory of Lovesey and Meserve. In this theory the sum rule and $\langle\omega_q^n\rangle$ for $n<6$ are also calculated self-consistently. A cutoff is introduced by assuming a three-pole line shape. This cutoff is rather weak and all higher moments for $n>6$ are therefore infinite. The parameter τ describing the central purely imaginary pole is not, in principle, determined from $\langle\omega_q^2\rangle$ and $\langle\omega_q^4\rangle$. However, Sears[19] suggested in the theory of liquids that τ could approximately be related to these moments and Lovesey[7] showed this correponds to using a Gaussian line shape for the random force relaxation function for large frequencies. In CT one needs near T_c a strong cutoff at quite low frequencies. This can only be obtained in the three-pole approximation by giving a large weight to the central pole. This results in the appearance of a central peak for which there is no evidence in EuO. It was, in fact, found independently[18] that the damped harmonic-oscillator (two-pole) line shape yields the best fit to the experimental data even at T_c.

However, the overall agreement between the results obtained here and in Ref. 11 and those obtained by the independent calculations by Young and Shastry[12] is a good test of both calculations, which differ considerably both in philosophy and in technical details.

ACKNOWLEDGMENTS

It is a pleasure to thank D. Yang and J. F. Cooke for discussions and help with some of the numerical calculations. The hospitality and financial support by the Solid State Division of the Oak Ridge National Laboratory is gratefully acknowledged. Thanks are also due to J. Als-Nielsen, L. Passell, H. A. Mook, and H. G. Bohn for discussions on the experimental results.

APPENDIX A: SOLVING THE GREEN'S-FUNCTION EQUATION

In order to solve the Green's-function equation (3) for small frequencies it is advantageous to reformulate the equation so that the fact that $G_2(\omega=0)\equiv 0$ is explicitly evident. For this purpose the equation of motion to second order for $G_2(\omega)$ was investigated in collaboration with Yang.[11] Using the exact relation between Green's functions and relaxation functions,

$$2\pi\langle\langle A,B\rangle\rangle_\omega=(A(t)B)_{t=0}+i\omega(AB)_\omega\ , \qquad \text{(A1)}$$

one finds, after some algebra, the exact equation

$$G_2(\omega)F_0(\omega)=-2\omega(\omega a_{10}+a_{20})(\omega+a_{21})G_0(\omega)+(\omega a_{10}+a_{20})[a_{10}(\omega+2a_{21})-a_{20}][G_0(0)-G_0(\omega)]$$
$$-\omega[b_{30}-b_{20}(\omega+2a_{21})+2b_{10}(a_{10}a_{21}-a_{20})]-i\omega(\omega+a_{21})^2(X_1X_1^\dagger)_\omega\,, \tag{A2}$$

where

$$F_0(\omega)=\omega^2+\omega a_{21}+a_{21}a_{10}-a_{20} \tag{A3}$$

is the same factor as that multiplying $G_0(\omega)$ in Eq. (3). Equation (A2) serves several purposes. First, it shows explicitly that $G_2(\omega=0)\equiv 0$, second, that $(X_1X_1^\dagger)_\omega$ does not have a singularity at zero frequency of the type ω^{-n} with $n\geq 1$, and third, that a part of the memory function $M(\omega)$ is explicitly known. By the memory-function technique one expresses $G_2(\omega)$ as $M(\omega)G_0(\omega)$. Inclusion of this explicit part of the memory function removes the δ-function singularity at $\omega^2=a_{20}$ found from Eq. (3) if $G_2(\omega)$ is simply neglected for $T>T_c$. Equation (A2) also shows that the solution of (3) together with (A2) does not depend on $(X_1X_1^\dagger)_\omega$ for $\omega=0$ and $-a_{21}$. At these most important frequencies the solution is therefore not sensitive to any approximations made in evaluating $(X_1X_1^\dagger)_\omega$. For $T>T_c$, $a_{21}=0$. Consequently, the two-pole solution is exact to order ω^2 for small frequencies. The result of this analysis was first mentioned in the short summary of the CT by the author and Yang in Ref. 11.

APPENDIX B: CUTOFF DETERMINED BY $\langle\omega_q^4\rangle$

Let us assume as the line-shape function, as cutoff harmonic oscillator form with poles $\pm\alpha+i\beta$ such that $a^2=\alpha^2+\beta^2$,

$$F(\omega)=\begin{cases}\dfrac{K}{\pi}\dfrac{1}{(\omega^2-a^2)^2+4\beta^2\omega^2} & \text{for } -\omega_c<\omega<\omega_c\\ 0 \text{ otherwise}\,.\end{cases} \tag{B1}$$

We require $F(\omega)$ to be normalized and to yield the correct moments $\langle\omega_q^n\rangle=\int_{-\infty}^{\infty}\omega^nF(\omega)d\omega$ for $n=2$ and 4. Direct integration yields

$$\omega_c=\frac{\pi}{2K}[\langle\omega_q^4\rangle-2(\alpha^2-\beta^2)\langle\omega_q^2\rangle+a^4]\,,$$
$$K=\begin{cases}4\pi\beta a^2\left\{\dfrac{\beta}{\alpha}\ln\left[\dfrac{\omega_c^2+2\alpha\omega_c+a^2}{\omega_c^2-2\alpha\omega_c+a^2}\right]+2\left[\arctan\left[\dfrac{\omega_c-\alpha}{\beta}\right]+\arctan\left[\dfrac{\omega_c+\alpha}{\beta}\right]\right]\right\}^{-1} & (\alpha^2>0)\\ \pi\alpha_1\left\{(\beta+\alpha_1)\arctan\left[\dfrac{\omega_c}{\beta-\alpha_1}\right]-(\beta-\alpha_1)\arctan\left[\dfrac{\omega_c}{\beta+\alpha_1}\right]\right\}^{-1} & (\alpha^2<0)\end{cases} \tag{B2}$$

$$\langle\omega^2\rangle=\begin{cases}a^2\left\{\dfrac{2K}{\pi}\left[\arctan\left[\dfrac{\omega_c+\alpha}{\beta}\right]+\arctan\left[\dfrac{\omega_c-\alpha}{\beta}\right]\right]-1\right\} & (\alpha^2\geq 0)\\ \left\{\dfrac{2\beta K}{\pi}\left[(\beta+\alpha_1)\arctan\left[\dfrac{\omega_c}{\beta-\alpha_1}\right]+(\beta-\alpha_1)\arctan\left[\dfrac{\omega_c}{\beta+\alpha_1}\right]\right]+(\alpha^2-\beta^2)\right\} & (\alpha^2<0)\end{cases}$$

where $\alpha\equiv i\alpha_1$ when $\alpha^2<0$. The equations are solved iteratively for α for fixed $\langle\omega^4\rangle$, $\langle\omega^2\rangle$, and β. When the cutoff frequency ω_c decreases from an infinite value the real part α^2 increases in order to satisfy the second moment. The larger value for α is used in (15) to determine a new larger characteristic halfwidth frequency Γ. When ω_c is large the correction of α is small and may be neglected. The fourth moment is

$$\langle\omega_q^4\rangle=\langle[L^2A,LA^\dagger]\rangle/\chi_q\,.$$

It was calculated for the Heisenberg model by Collins and Marshall.[3] For NN interaction it consists of terms of the type

$$J^3 \sum_{A,B,C} (1-e^{iqA})(1-e^{-iqC})\langle S_0^x S_A^x S_{A+B}^z S_{B+C}^z \rangle / \chi_q ,$$

where A, B, and C are NN vectors. The four-spin correlation function is decoupled into pairs in analogy to the mode-mode decoupling. The temperature dependence of the NN correlation function is simply related to the second moment. We write

$$\langle S_0 S_R \rangle_T = \sum_k \gamma_k \langle S_k S_{-k} \rangle = \chi_{q_z} \langle \omega_{q_z}^2 \rangle / 4J_0 ,$$

where $\gamma_k = J_k / J_0$ and q_z is the (111) zone-boundary wave for the fcc structure. Terms of the type $\langle S_0^x S_0^z S_R^x S_R^z \rangle_T$ are not decoupled but calculated as

$$\langle S_0^x S_0^z S_R^x S_R^z \rangle_\infty \langle S_0 S_R \rangle_T / \langle S_0 S_R \rangle_\infty .$$

This real-space method yields the exact $\langle \omega_q^4 \rangle$ at $T=\infty$ and the summation over the NN vectors is rapid to perform. The method can now be generalized to further neighbor interactions. In previous calculations $\langle \omega_q^4 \rangle$ has been decoupled in q space which gives rise to an additional summation over all wave vectors and it is not possible to reproduce exactly $\langle \omega_q^4 \rangle$ at $T=\infty$. Since $\langle \omega_q^4 \rangle$ is only used to determine the cutoff frequency ω_c, the final results are not very sensitive to approximations in $\langle \omega_q^4 \rangle$.

---

*Permanent address.

[1]D. N. Zubarev, Usp. Fiz. Nauk 71, 71 (1960) [Sov. Phys.—Usp. 3, 320 (1960)].

[2]H. Mori, Prog. Theor. Phys. 33, 432 (1965); 34, 399 (1965); K. Kawasaki, *ibid.* 39, 1133 (1968); 40, 11 (1968).

[3]P. G. De Gennes, J. Phys. Chem. Solids 4, 223 (1958).

[4]R. Resibois and M. De Leener, Phys. Rev. 152, 305 (1966).

[5]H. Tomita and H. Mashiyama, Prog. Theor. Phys. 45, 1407 (1971).

[6]M. Blume and J. Hubbard, Phys. Rev. B 1, 3815 (1970); J. Hubbard, J. Phys. C 4, 53 (1971).

[7]S. W. Lovesey and R. A. Meserve, J. Phys. C 6, 79 (1973).

[8]L. Passell, O. W. Dietrich, and J. Als-Nielsen, Phys. Rev. B 14, 4897 (1976); J. Als-Nielsen, O. W. Dietrich, and L. Passell, *ibid.* 14, 4908 (1976); O. W. Dietrich, J. Als-Nielsen, and L. Passel, *ibid.* 14, 4923 (1976).

[9]H. G. Bohn, W. Zinn, B. Dorner, and A. Kollmar, Phys. Rev. B 22, 5447 (1980); J. Appl. Phys. 52, 2228 (1981).

[10]T. R. McGuire and M. W. Schafer, J. Appl. Phys. 35, 984 (1964).

[11]P. A. Lindgård, J. Appl. Phys. 53, 1861 (1982); P. A. Lindgård and D. Yang, J. Magn. Magn. Mater. 15–18, 1037 (1980); P. A. Lindgård, in *Crystalline Electric Field and Structural Effects in f-Electron Systems,* edited by J. E. Crow (Plenum, New York, 1980).

[12]P. Young and Shastry, J. Phys. C 15, 4547 (1982).

[13]M. F. Collins and W. Marshall, Proc. Phys. Soc. London 92, 390 (1967).

[14]P. A. Lindgård, in Proceedings of the ICM, Japan, 1982 [J. Magn. Magn. Mater. (in press)].

[15]For a review, see V. L. Ginzburg, A. P. Levanyuk, and A. A. Sobyanin, Phys. Rep. 57, 151 (1980).

[16]G. S. Rushbrooke, G. A. Baker, Jr., and P. J. Wood, in *Phase Transitions and Critical Phenomena,* edited by C. Domb and M. S. Green (Academic, New York, 1974), Vol. 3.

[17]A. D. Bruce and A. Aharony, Phys. Rev. B 10, 2078 (1974).

[18]H. A. Mook, Phys. Rev. Lett. 46, 508 (1981).

[19]V. F. Sears, Can. J. Phys. 47, 199 (1969).